Parameter Estimation of Photovoltaic Cells using Transit Search Optimizer

Hady El Said Abdel Maksoud
Department of Electrical Engineering, College of Engineering, Northern Border University, Saudi Arabia | Electrical Engineering Department, Faculty of Engineering, Menoufia University, Egypt
hady.elgendy@nbu.edu.sa

Shaaban M. Shaaban
Department of Electrical Engineering, College of Engineering, Northern Border University, Saudi Arabia | Department of Engineering Basic Science, Faculty of Engineering, Menoufia University, Egypt
shabaan27@gmail.com

Received: 23 January 2024 | Revised: 17 February 2024, 7 March 2024, and 17 March 2024 | Accepted: 24 March 2024

 DOI: https://doi.org/10.48084/etasr.6956

ABSTRACT

In the evaluation of a Photovoltaic (PV) system's performance, precise calculation of the system's parameters is essential, as these parameters significantly influence its efficiency across various sunlight intensities, temperature ranges, and distinct load conditions. Addressing the intricate non-linear optimization problem of pinpointing these PV system parameters, the current research adopts a novel metaheuristic optimization approach, called Transit Search (TS). The proposed technique was rigorously tested on a monocrystalline solar panel, which included both single and double-diode model structures. The design of the objective function within this framework aims to diminish the square root of the average squared discrepancies between theoretical and measured current outputs, while remaining within the established parameter bounds. The proficiency of the TS algorithm was highlighted by employing a variety of statistical error indicators, underlining the latter's effectiveness. When pitted against other established optimization algorithms through comparative analysis, TS demonstrated outstanding capabilities, evidently outperforming its contemporaries in the accurate determination of PV system parameters.

Keywords-parameter extraction; PV cells; modeling; TS algorithm; optimization

I. INTRODUCTION

Accurate determination of the parameters of solar photovoltaic (PV) models is a linchpin for the precise projection of the panels' performance and efficiency [1]. It enables the fine-tuning of the solar panels' architecture, their functioning, and their seamless incorporation into broader energy systems to ensure optimal energy harvest and efficiency [2]. Moreover, meticulous parameter estimation is instrumental in the health assessment and prognostics of these systems, paving the way for preventative maintenance, prolonged service life, and steady energy output. This, in turn, fortifies the economic and operational viability of solar power installations [3]. Technical specifications of PV modules conventionally underscore three salient points delineating the current/voltage (I/V) characteristics under Standardized Test Conditions (STC), i.e. ambient temperature T of 25°C, solar irradiance G of 1 kW/m^2, and air mass coefficient of 1.5. These benchmarks include the open-circuit voltage (V_{oc}), the short-circuit current (I_{sc}), and the maximum power point's voltage (V_{mp}) and current (I_{mp}) [4]. Yet, such data points, while indicative, are not comprehensive enough for extensive PV systems analysis, given the dynamic nature of environmental conditions. An exhaustive and precise I/V curve, relevant across the entire spectrum of operational conditions, is vital for an in-depth assessment of PV systems' performance.

The electrical behavior of PV cells is commonly depicted using two models: the One-Diode Model (ODM) and the Dual-Diode Model (DDM). The DDM, although more resource-intensive than the ODM, offers only a slight edge in efficiency [5]. The ODM requires the identification of five key parameters, whereas the DDM necessitates seven. Additionally, the Triple Diode Model (TDM) further refines this by more accurately representing recombination losses across a wider range of conditions, albeit with increased complexity and computational demands. This study concentrates primarily on the ODM and DDM [6].

The study of solar cell dynamics frequently employs the ODM and the DDM [7]. For the enhancement of PV system efficiency via simulation analysis, precise estimation and delineation of model parameters are crucial. There is a significant research thrust aimed at honing PV model parameters through various engineering methods [8]. These methods fall into two primary classifications from an algorithmic perspective: deterministic and heuristic. Both

methodologies are oriented towards converting the task of parameter determination into an optimization problem, utilizing certain benchmarks derived from the I/V characteristic curve [8, 9].

Deterministic strategies often implement techniques like the Newton method-based least squares and Lambert W-functions, which impose requirements on objective functions related to continuity, convexity, and the presence of derivatives [10]. However, these approaches can be affected by initial conditions and details regarding the gradient, leaving them vulnerable to entrapment in local optima during complex optimization problems. This can be a significant limitation in non-linear and multimodal tasks of parameter extraction. Conversely, heuristic methods boast adaptability, not being restricted by the stringent specifications of the optimization problem's framework. This adaptability grants them an advantage in overcoming the challenges posed by initial conditions and gradient specifications. Due to their robustness, heuristic methods have gained traction. Techniques like Genetic Algorithms (GAs) [11], Particle Swarm Optimization (PSO) [12], differential evolution [13], Artificial Bee Colony (ABC), and harmony search [15] are just a few of the heuristic approaches that have been successfully applied to PV model parameter optimization. Additional methods include teaching–learning-based optimization [16], the chaotic whale optimization algorithm [17], Lévy flight trajectory-based whale optimization [18], and hybrid algorithms that combine features of different optimization methods.

This research paper introduces substantial advancements in solar energy, particularly through the innovation of parameter identification processes for solar PV models via a novel optimization algorithm. It heralds the inaugural application of the Transit Search (TS) algorithm, meticulously adapted for the precise optimization of PV cell parameters. This pioneering effort not only enriches the existing body of knowledge but also sets a new benchmark for future research in solar energy optimization techniques. The TS algorithm is utilized for extracting parameters of PV cells [19]. This algorithm is an innovative optimization method influenced by astrophysics. It is a meta-heuristic algorithm, rooted in the transit method, which has proven effective in the discovery of exoplanets through space telescopes. At its core, the TS algorithm emulates the technique of detecting planets by observing fluctuations in starlight. We have conducted a comprehensive comparative study for PV cell parameters. This study considered both ODM and DDM (Tables I, III), utilizing six advanced optimization algorithms: Nelder-Mead and modified PSO (NM-MPSO) [20], ABC optimization [21], improved adaptive differential evolution (Rcr-IJADE) [22], Artificial Bee Swarm Optimization (ABSO) algorithm [23], Levenberg-Marquardt algorithm combined with Simulated Annealing (LMSA) [24], and Chaotic Asexual Reproduction Optimization (CARO) [25]. These methodologies were meticulously chosen for their relevance and potential to provide insightful comparisons.

II. MODELING OF PV CELLS

A. One-Diode Model

ODM, often referred to as the single diode model or the diode model, is a prevalent mathematical framework for capturing the electrical characteristics of a PV cell.

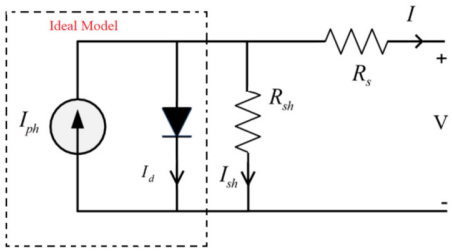

Fig. 1. The one-diode model.

$$I = I_{ph} - I_d - I_{sh} \quad (1)$$

with $I_d = I_{sd}\left(e^{\left(\frac{q(V+R_sI)}{\alpha KT}\right)}-1\right)$ and $I_{sh} = \frac{(V+R_sI)}{R_{sh}}$. This formula describes the variation of the output current I in a PV cell relative to the applied voltage V considering several key factors. These include the photocurrent (I_{ph}), the diode current (I_d), the shunt current (I_{sh}), representing the current that flows through the shunt resistor in parallel with the diode, and the reverse saturation current (I_{sd}), along with the diode ideality factor (α). It also factors in the temperature T of the cell, the Boltzmann constant K, the charge of an electron q, and the impacts of both series (R_s) and shunt resistance (R_{sh}).

B. Dual-Diode Model

DDM, is an advanced mathematical representation used to describe the electrical behavior of PV cells.

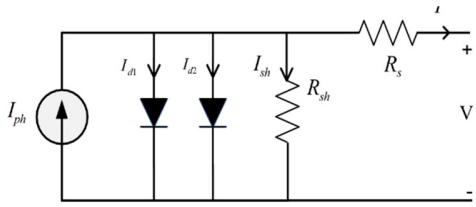

Fig. 2. The dual-diode model.

$$I = I_{ph} - I_{d1} - I_{d2} - I_{sh} \quad (2)$$

with $I_{d1} = I_{sd1}\left(e^{\left(\frac{q(V+R_sI)}{\alpha_1 KT}\right)}-1\right)$ and $I_{d2} = I_{sd2}\left(e^{\left(\frac{q(V+R_sI)}{\alpha_2 KT}\right)}-1\right)$.

The characteristics of the second diode are: the diode current (I_{d2}), the reverse saturation current (I_{sd2}) and the diode ideality factor (α_2).

C. Objective Function

In the process of deriving parameters for PV cells, the objective functions act as crucial mathematical benchmarks that steer the optimization procedures. This entails aligning the theoretically calculated current values with those obtained from real-world experiments. Central to accomplishing this alignment is the employment of an objective function, specifically designed to reduce the Root Mean Square Error (RMSE) over a range of gathered data points [26]. The primary equation used to compute the RMSE, which measures the discrepancy between observed and predicted current values, is:

$$\text{RMSE} = \sqrt{\frac{1}{N}\left(\sum_{i=1}^{N}\left(I_m - I_e\right)\right)^2} \quad (3)$$

where N is the number of samples, I_m denotes the measured current, and I_e represents the estimated current.

The purpose of using the objective function is predominantly to minimize the RMSE over various collected data points. Essentially, this involves reducing the difference between the model's predicted values and the actual experimental observations. For the ODM, the objective function is structured as:

$$f_{ODM} = \sqrt{\frac{1}{N}\left(\sum_{i=1}^{N}\left(I_m - I_{ph} + I_{sd1}\left[e^{\left(\frac{q(V+R_sI)}{\alpha_1 KT}\right)} - 1\right] + \frac{V+R_sI}{R_{sh}}\right)\right)^2} \quad (4)$$

Conversely, when considering the DDM, (5) represents the error function:

$$f_{DDM} = \sqrt{\frac{1}{N}\left(\sum_{i=1}^{N}\left(\begin{array}{l} I_m - I_{ph} + I_{sd1}\left[e^{\left(\frac{q(V+R_sI)}{\alpha_1 KT}\right)} - 1\right] \\ +I_{sd2}\left[e^{\left(\frac{q(V+R_sI)}{\alpha_2 KT}\right)} - 1\right] + \frac{V+R_sI}{R_{sh}} \end{array}\right)\right)^2} \quad (5)$$

III. TRANSIT SEARCH ALGORITHM

TS is a meta-heuristic algorithm that draws its principles from the transit method, a successful approach in detecting exoplanets via space telescopes. In essence, the TS algorithm mimics the process of identifying planets through the observation of changes in stellar luminosity. In astrophysics, this method involves studying the light from stars at regular intervals to detect any reduction in brightness, which could indicate a planet passing in front of the star. Similarly, the TS algorithm applies this concept to optimization problems. It systematically explores potential solutions by monitoring changes in some "luminosity" equivalent, which represents the quality or fitness of the solution. When a decrease in this value is observed, it suggests a potential "transit" or optimal solution crossing the problem space, akin to a planet transiting a star. The implementation of the TS algorithm comprises five distinct phases: galaxy, star, transit, planet, neighbor, and exploitation [19].

A. Galaxy Phase

The algorithm initiates by selecting a galaxy through the choice of a random point in the search space, designated as the center of the galaxy. Following this, it is crucial to pinpoint the habitable zones within this galaxy, often referred to as the life belt. This is achieved by evaluating n_s*SN random regions. The number of host stars (n_s) and the signal-to-noise ratio (SN), denoted as L_R, using (6)-(8):

$$L_{R,l} = L_{Galaxsy} + D - Noise \text{ with } l = 1,...,(n_s \times SN) \quad (6)$$

In which:

$$D = \begin{cases} c_1 L_{Galaxsy} - L_r & \text{if } z = 1 \text{ (Negative region)} \\ c_1 L_{Galaxsy} + L_r & \text{if } z = 2 \text{ (Positive region)} \end{cases} \quad (7)$$

$$Noise = (c_2)^3 L_r \quad (8)$$

In the previously referenced equations, L_{Galaxy} signifies the central position of the galaxy. Additionally, L_r denotes a randomly selected point within the search space. The equations also incorporate two coefficients, both ranging from 0 to 1: one is a random scalar (c_1) and the other is a random vector (c_2), the dimensions of which correspond to the number of variables in the optimization problem. Following this, the next step involves selecting a star from each of the chosen regions, representing a stellar system, as per (9)-(11). Consequently, at this stage's conclusion, the algorithm possesses n_s stars for exploration. The position of these stars is denoted by L_s in (9). The coefficients c_3 and c_4 in these equations are random values ranging between 0 and 1, while coefficient c_5 is a random vector also confined between 0 and 1.

$$L_{S,i} = L_{R,i} + D - Noise \text{ with } i = 1,...,n_s \quad (9)$$

In which:

$$D = \begin{cases} c_4 L_{R,i} - c_3 L_r & \text{if } z = 1 \text{ (Negative region)} \\ c_4 L_{R,i} + c_3 L_r & \text{if } z = 2 \text{ (Positive region)} \end{cases} \quad (10)$$

$$Noise = (c_5)^3 L_r \quad (11)$$

In the algorithm outlined, the galaxy phase is conducted a single time, preceding the commencement of iterative processes. This phase is crucial for selecting suitable scenarios in which the core steps of the algorithm (phases 2 through 5) can be effectively executed.

B. Transit Phase

In the TS algorithm, determining the class of each star is based on its brightness, according to the definition provided in $M2$. For instance, [19] showcases a search space example featuring eight stars, each ranked for a minimization goal. In this scenario, the closer the star is to the observer, the more photons are received. This principle is encapsulated in (12) of the proposed algorithm, which approximates the star's luminosity.

$$L_i = \frac{R_i / n_s}{(d_i)^2} \qquad i = 1,...,n_s \quad R_i \in \{1,...,n_s\} \tag{12}$$

$$d_i = \sqrt{(L_S - L_T)^2} \qquad i = 1,...,n_s \tag{13}$$

L_i and R_i represent the luminosity and rank of a given star, denoted as star *i*. Additionally, d_i, pertains to the distance from the telescope to star *i*. The initial position of the telescope, indicated by L_T, is determined randomly at the beginning of the algorithm and remains constant throughout the optimization process. To update the amount of light received from the star, a new signal is generated by modifying L_S, in accordance with the principles defined in M_2. This adjustment utilizes (14), (15). Within this framework, the coefficients c_6 and c_7 are assigned values randomly, $c6$ is chosen from a range of -1 to 1, while c_7 is selected as a random vector within the range of 0 to 1.

$$L_{S,new,i} = L_{S,i} + D - Noise \qquad i = 1,...,n_s \tag{14}$$

In which:

$$\begin{cases} D = c_6 L_{S,i} \\ Noise = (c_7)^3 L_S \end{cases} \tag{15}$$

The star's brightness level is computed (utilizing the newly acquired f_s from the updated $L_{S,new}$), leading to the determination of the new luminosity value, $L_{i,new}$, as specified in (16):

$$L_{i,new} = \frac{R_{i,new} / n_s}{(d_{i,new})^2} \qquad i = 1,...,n_s \tag{16}$$

The new parameter $d_{i,new}$ is calculated using the updated L_S and the telescope's position. By comparing L_i and $L_{i,new}$, the potential for a transit event can be assessed. This likelihood, represented by P_T, is expressed as either 1 (indicating a probability of transit) or 0 (signifying no transit), as defined in (17). If P_T equals 1, the algorithm employs the planet phase; if not, the neighbor phase is applied in the current iteration.

$$\begin{cases} if \quad L_{i,new} < L_i & P_T = 1 \text{ (Transit)} \\ if \quad L_{i,new} \geq L_i & P_T = 0 \text{ (No Transit)} \end{cases} \tag{17}$$

C. Planet Phase

When the value of P_T, as established in the preceding phase, indicates a transit (P_T = 1), the planet phase is activated within the TS algorithm. This phenomenon aids in ascertaining the initial location of the detected planet (L_z). The TS algorithm calculates this position following the methodology outlined in (18):

$$L_z = (c_8 L_T + R_L L_{S,i}) / 2 \quad i = 1,...,n_s \tag{18}$$

where $R_L = L_{S,new,i} / L_{S,i}$. The parameter R_L signifies the luminance ratio. The coefficient c_8 assumes a random value within the range of 0 to 1. Equation (18) establishes the position of a planet situated between a star and a telescope by averaging the two relative locations.

The *SN* plays a pivotal role in transit confirmation and noise reduction. To determine the planet's approximate location, the algorithm evaluates the number of received signals within its stellar system. Equation (19) considers a set of *SN* signals for this purpose, with the coefficient c_9 being a random number ranging from -1 to 1. Furthermore, c_{10} is a random vector with values spanning from -1 to 1. Following the determination of signals (L_m), (20) is employed to refine the final location of the detected planet ( ) by taking the average of the *SN* signals.

$$L_{m,j} = \begin{cases} L_z + c_9 L_r & \text{if } z = 1 \quad \text{Aphelion region} \\ L_z - c_9 L_r & \text{if } z = 2 \quad \text{Perihelion region} \\ L_z + c_{10} L_r & \text{if } z = 3 \quad \text{Neutral region} \end{cases} \quad j = 1,...,SN \tag{19}$$

$$L_P = \frac{\sum_{j=1}^{SN} L_{m,j}}{SN} \tag{20}$$

D. Neighbor Phase

In cases where there is no transit observed for a star during the current observation, the TS algorithm proceeds to investigate neighboring planets of the previously detected star. This substitution occurs during the neighbor phase, utilizing (21)-(23). To begin, the initial location of the neighbor (L_z) is estimated by (21), taking into account its host star ($L_{S,new}$) and a random location (L_R). The final location of the neighbor planet (L_N) is determined using (22) and (23). The coefficients c_{11} and c_{12} in (21) correspond to random numbers falling within the range of 0 to 1. Additionally, the coefficients c_{13} and c_{14} in (22) represent a random number and a vector ranging from -1 to 1:

$$L_z = (c_{11} L_{s,new} + c_{12} L_r) / 2 \tag{21}$$

$$L_{n,j} = \begin{cases} L_z - c_{13} L_r & \text{if } z = 1 \text{ Aphelion region} \\ L_z + c_{13} L_r & \text{if } z = 2 \text{ Perihelion region} \\ L_z + c_{14} L_r & \text{if } z = 3 \text{ Neutral region} \end{cases} \quad j = 1,...,SN \tag{22}$$

$$L_{N,i} = \frac{\sum_{j=1}^{SN} L_{m,j}}{SN} \tag{23}$$

E. Exploitation Phase

In the preceding phases, the optimal planet is selected for each star. However, the mere discovery of a planet is not sufficient. It is essential to thoroughly examine the planet's characteristics and its potential to support life. The TS algorithm addresses this in the exploitation phase, where a fresh definition of L_P is introduced. Here, L_P in the current phase (L_E) represents the attributes of the planet, encompassing factors like density, composition, atmosphere, and more. Subsequently, by incorporating new knowledge (*K*), the planet's characteristics are adjusted *SN* times (j = 1,. . . , *SN*) using (24) and (25). In (25), c_{15} is a random number ranging from 0 to 2, while c_{16} falls within the range of 0 to 1. Additionally, c_{17} is a random vector with values between 0 and 1. The parameter *P* in (25) denotes a random exponent ranging from 1 to (ns * *SN*). c_k represents a random number (1, 2, 3, or

4) indicating the knowledge index. Four states are considered for c_k in the TS algorithm.

$$L_{E,j} = \begin{cases} c_{16}L_P + c_{15}K & if \quad c_k = 1 \quad (\text{state 1}) \\ c_{16}L_P - c_{15}K & if \quad c_k = 2 \quad (\text{state 2}) \\ L_p - c_{15}K & if \quad c_k = 3 \quad (\text{state 3}) \\ L_p + c_{15}K & if \quad c_k = 4 \quad (\text{state 4}) \end{cases} \tag{24}$$

$$K = (c_{17})^P L_r \tag{25}$$

The stages of the TS algorithm, including their definitions and specifics, accompanied by pertinent equations and pseudocodes can be found in [19].

To optimize PV cell parameters using the TS algorithm, the key parameters that need tuning include:

- V_{min} and V_{max}: These vectors set the lower and upper bounds for the variables, ensuring the search is within realistic limits.
- n_V: The number of variables (PV parameters) to optimize, set to 5 for OMD and to 7 for DDM.
- n_s (number of stars): Influences the algorithm's exploratory scope, set here as 10 to balance exploration and computational efficiency.
- *SN*: Determines the granularity of the search, with a value of 10 providing a detailed yet manageable exploration.
- *maxcycle*: The maximum number of iterations the algorithm will perform, set to 1500, allowing sufficient convergence time for the optimization process.

These parameters directly correlate with the optimization process's efficiency and accuracy in extracting PV cell parameters. Tuning them involves adjusting the search space's bounds, the granularity of the search, and the algorithm's runtime to effectively navigate the complex landscape of PV parameter optimization.

IV. RESULTS AND DISCUSSION

The extraction of various simulation results was facilitated using specific software and hardware. The setup included an Intel (R) Core (TM) i7 – 7500U CPU operating at 2.9 GHz, 12 GB RAM, Matlab R2022b for simulation, and Windows 11 as the operating system. Simulations were performed under uniform environmental conditions, with a solar irradiance of 1000 W/m^2 and a cell temperature of 33 °C. These were applied to the RTC France Company's monocrystalline PV panel [27], utilizing both single and double diode cell models to ensure comprehensive analysis. The statistical metrics used to demonstrate the performance of the proposed algorithm are Individual Absolute Error (IAE), Median Absolute Error (MAE), and Residual Sum of Squares (SSE):

$$\text{IAE} = \left| I_{measured} - I_{estimated} \right|$$

$$\text{MAE} = \sum_{i=1}^{m} \frac{\left| I_{measured} - I_{estimated} \right|}{m}$$

$$\text{SSE} = \sum_{i=1}^{m} \left(I_{measured} - I_{estimated} \right)^2$$

Table I displays the performance metrics for the TS algorithm applied to ODM parameter extraction, benchmarked against other techniques.

TABLE I. PARAMETER EXTRACTION FOR ODM

Algorithm	I_{ph} (A)	I_0 (μA)	α	R_s (Ω)	R_{sh} (Ω)
TS	0.76078	0.293558	1.4716	0.0368	51.6718
BBO-M	0.760781	0.318743	1.479842	0.036422	53.36226
RADE	0.760775	0.323022	1.481183	0.036376	53.71853
LMSA	0.760781	0.318492	1.479764	0.036433	53.32644
CARO	0.760792	0.317243	1.481681	0.036443	53.0893
ABC	0.76082	0.325155	1.481731	0.036443	53.64332
NM-MPSO	0.760781	0.323065	1.481202	0.036384	53.72221

Figures 3 and 4 demonstrate that the TS algorithm generally exhibits superior performance in parameter extraction for the ODM, with the lowest SSE and RMSE. These results suggest that TS is highly accurate and consistent in its predictions compared to the other evaluated algorithms. Figure 5 shows a comparison of the estimated and the actual results of the TS algorithm for the DDM case.

	NM-MPSO	ABC	LMSA	CARO	BBO-M	RADE	TS
IAT	1.77E-02	2.05E-02	2.15E-02	1.82E-02	2.13E-02	1.77E-02	1.73E-02
RMSE	9.83E-04	1.04E-03	9.86E-04	9.87E-04	9.86E-04	9.86E-04	9.20E-04
SSE	2.51E-05	2.84E-05	2.53E-05	2.53E-05	2.528E-05	2.528E-05	2.20E-05
MAE	6.81E-04	7.88E-04	8.27E-04	6.98E-04	8.19E-04	6.81E-04	6.65E-04

Fig. 3. Statistical results for the ODM.

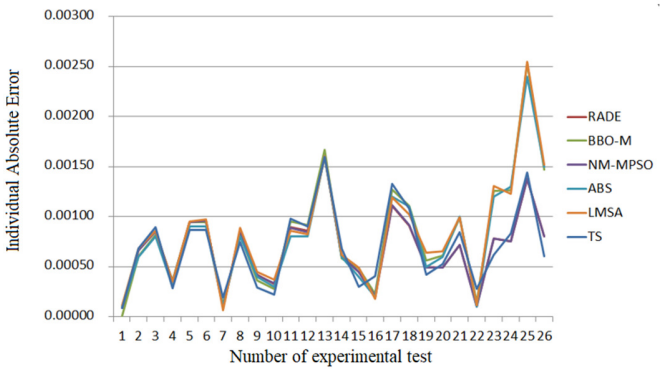

Fig. 4. Individual-Absolute Error (IAE) obtained for the ODM.

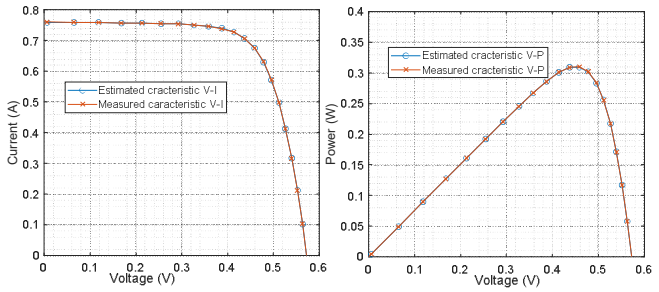

Fig. 5. Experimental and estimated results obtained by the TS algorithm for DDM.

Table II presents a comparative analysis of the performance indicators for DDM parameter extraction.

TABLE II. PARAMETER EXTRACTION FOR DDM

Algorithm	I_{ph} (A)	I_{01} (μA)	I_{02} (μA)	α_1	α_2	R_s (Ω)	R_{sh} (Ω)
TS	0.760723	0.22766	0.63012	1.427	1.806	0.0472	54.7972
RADE	0.760781	0.22597	0.749347	1.45101	2	0.03674	55.4854
CARO	0.760752	0.29315	0.090982	1.47338	1.77322	0.03641	54.3967
ABSO	0.76078	0.26713	0.38191	.146512	1.98152	0.03657	54.6219
ABC	0.760825	0.04071	0.287433	1.44954	1.48852	0.03645	54.7805
NM-MPSO	0.76078	0.22476	0.75524	1.45054	1.99998	0.03675	55.5296

Figures 6 and 7 provide statistical results and a graphical representation of the IAE for various optimization algorithms applied to the DDM. The following conclusions can be drawn:

- The TS algorithm has the lowest total IAE, indicating it has the smallest overall prediction error compared to the other algorithms.
- The TS algorithm consistently maintains lower error values across most data points (Figure 7), reinforcing the data from Figure 6 about its accuracy and reliability.
- There is a notable spike in errors for all algorithms at data point 22 (Figure 7), suggesting a particularly challenging case for parameter estimation. However, TS still has one of the lowest errors at this point.

	NM-MPSO	ABC	ABSO	CARO	RADE	TS
Total IAE	1.74E-02	2.04E-02	1.78E-02	6.93E-02	1.77E-02	1.71E-02
RMSE	9.83E-04	1.04E-03	9.83E-04	9.83E-04	9.82E-04	9.20E-04
SSE	2.51E-05	2.79E-05	2.51E-05	2.51E-05	2.51E-05	2.21E-05
MAE	6.68E-04	7.84E-04	6.83E-04	2.67E-03	6.81E-04	6.57E-04

Fig. 6. Statistical results for the DDM.

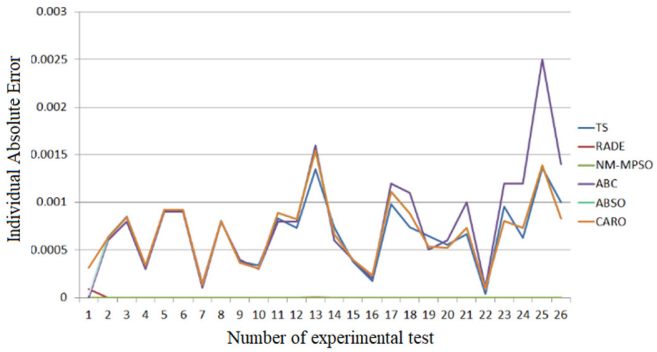

Fig. 7. IAE obtained for DDM.

According to the presented results in Figures 5 and 8, it can be noticed that the estimated current coincides with the measured current, indicating the accuracy of the proposed optimization algorithm for parameters extraction. Figure 9 shows the DDM converging more rapidly and stabilizing at a lower error compared to the ODM. Both models eventually reach a plateau, indicating that optimal parameters have likely been achieved.

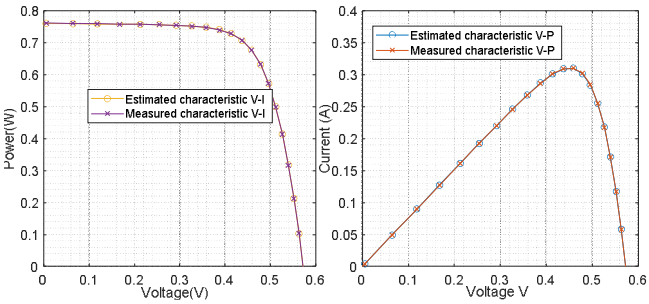

Fig. 8. Experimental and estimated results obtained by the TS algorithm for ODM.

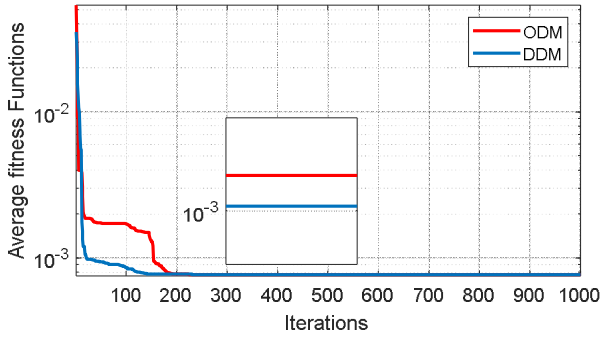

Fig. 9. Average fitness functions.

V. CONCLUSION

The findings of our research firmly establish the Transit Search (TS) algorithm as a powerful metaheuristic for parameter optimization in photovoltaic (PV) systems, characterized by its precision and reliability. The TS algorithm outperforms in estimating parameters for both the One-Diode and Dual-Diode Models and excels when assessed through various error metrics such as Root Mean Square Error (RMSE) and Sum of Squares Error (SSE). Comparative statistical analysis indicates that TS algorithm secures the most favorable error metrics in contrast to other established optimization algorithms, including NM-MPSO, ABC, ABSO, and CARO. However, while the TS algorithm's advantages in parameter estimation and error minimization are clear, potential limitations such as computational complexity and scalability in larger systems should be acknowledged.

ACKNOWLEDGMENT

The authors gratefully acknowledge the approval and support of this study by grant no. ENGA-2022-11-1396 from the Deanship of Scientific Research at Northern Border University, Arar, KSA.

REFERENCES

[1] Y. Abou Jieb, E. Hossain, and E. Hossain, *Photovoltaic systems: fundamentals and applications*. Springer, 2022.

[2] H. Kraiem *et al.*, "Parameters Identification of Photovoltaic Cell and Module Models Using Modified Social Group Optimization Algorithm," *Sustainability*, vol. 15, no. 13, Jan. 2023, Art. no. 10510, https://doi.org/10.3390/su151310510.

[3] T. Zhou and C. Shang, "Parameter identification of solar photovoltaic models by multi strategy sine–cosine algorithm," *Energy Science & Engineering*, vol. 2024, Jan. 2024, https://doi.org/10.1002/ese3.1673.

[4] F. Hu, S. Mou, S. Wei, Liping Qiu, H. Hu, and H. Zhou, "Research on the evolution of China's photovoltaic technology innovation network from the perspective of patents," *Energy Strategy Reviews*, vol. 51, Jan. 2024, Art. no. 101309, https://doi.org/10.1016/j.esr.2024.101309.

[5] I. Tebbal and A. F. Hamida, "Effects of Crossover Operators on Genetic Algorithms for the Extraction of Solar Cell Parameters from Noisy Data," *Engineering, Technology & Applied Science Research*, vol. 13, no. 3, pp. 10630–10637, Jun. 2023, https://doi.org/10.48084/etasr.5417.

[6] C. S. Sundar Ganesh, C. Kumar, M. Premkumar, and B. Derebew, "Enhancing photovoltaic parameter estimation: integration of non-linear hunting and reinforcement learning strategies with golden jackal optimizer," *Scientific Reports*, vol. 14, no. 1, Feb. 2024, Art. no. 2756, https://doi.org/10.1038/s41598-024-52670-8.

[7] R. M. A. Qasem and S. M. Massadeh, "Solving Cell Placement Problem Using Harmony Search Algorithms," *Engineering, Technology & Applied Science Research*, vol. 8, no. 4, pp. 3172–3176, Aug. 2018, https://doi.org/10.48084/etasr.2113.

[8] K. Njeh, M. A. Zdiri, M. B. Ammar, A. Rabhi, and F. B. Salem, "Energy Management of an Autonomous Photovoltaic System under Climatic Variations," *Engineering, Technology & Applied Science Research*, vol. 13, no. 1, pp. 9849–9854, Feb. 2023, https://doi.org/10.48084/etasr.5375.

[9] T. Soga, "Chapter 1 - Fundamentals of Solar Cell," in *Nanostructured Materials for Solar Energy Conversion*, T. Soga, Ed. Amsterdam, Netherlands: Elsevier, 2006, pp. 3–43.

[10] X. Gao, Y. Cui, J. Hu, G. Xu, and Y. Yu, "Lambert *W*-function based exact representation for double diode model of solar cells: Comparison on fitness and parameter extraction," *Energy Conversion and Management*, vol. 127, pp. 443–460, Nov. 2016, https://doi.org/10.1016/j.enconman.2016.09.005.

[11] J. A. Jervase, H. Bourdoucen, and A. Al-Lawati, "Solar cell parameter extraction using genetic algorithms," *Measurement Science and Technology*, vol. 12, no. 11, Jul. 2001, Art. no. 1922, https://doi.org/10.1088/0957-0233/12/11/322.

[12] M. Merchaoui, A. Sakly, and M. F. Mimouni, "Particle swarm optimisation with adaptive mutation strategy for photovoltaic solar cell/module parameter extraction," *Energy Conversion and Management*, vol. 175, pp. 151–163, Nov. 2018, https://doi.org/10.1016/j.enconman.2018.08.081.

[13] C. Chellaswamy and R. Ramesh, "Parameter extraction of solar cell models based on adaptive differential evolution algorithm," *Renewable Energy*, vol. 97, pp. 823–837, Nov. 2016, https://doi.org/10.1016/j.renene.2016.06.024.

[14] X. Chen, B. Xu, C. Mei, Y. Ding, and K. Li, "Teaching–learning–based artificial bee colony for solar photovoltaic parameter estimation," *Applied Energy*, vol. 212, pp. 1578–1588, Feb. 2018, https://doi.org/10.1016/j.apenergy.2017.12.115.

[15] W.-Y. Lee, S.-M. Park, and K.-B. Sim, "Optimal hyperparameter tuning of convolutional neural networks based on the parameter-setting-free harmony search algorithm," *Optik*, vol. 172, pp. 359–367, Nov. 2018, https://doi.org/10.1016/j.ijleo.2018.07.044.

[16] Z. Liao, Z. Chen, and S. Li, "Parameters Extraction of Photovoltaic Models Using Triple-Phase Teaching-Learning-Based Optimization," *IEEE Access*, vol. 8, pp. 69937–69952, 2020, https://doi.org/10.1109/ACCESS.2020.2984728.

[17] D. Prasad, A. Mukherjee, and V. Mukherjee, "Chapter 17 - Transient Stability Constrained Optimal Power Flow Using Chaotic Whale Optimization Algorithm," in *Handbook of Neural Computation*, P. Samui, S. Sekhar, and V. E. Balas, Eds. Cambridge, MA, USA: Academic Press, 2017, pp. 311–332.

[18] Y. Ling, Y. Zhou, and Q. Luo, "Lévy Flight Trajectory-Based Whale Optimization Algorithm for Global Optimization," *IEEE Access*, vol. 5, pp. 6168–6186, 2017, https://doi.org/10.1109/ACCESS.2017.2695498.

[19] M. Mirrashid and H. Naderpour, "Transit search: An optimization algorithm based on exoplanet exploration," *Results in Control and Optimization*, vol. 7, Jun. 2022, Art. no. 100127, https://doi.org/10.1016/j.rico.2022.100127.

[20] N. F. Abdul Hamid, N. Abd Rahim, and J. Selvaraj, "Solar cell parameters identification using hybrid Nelder-Mead and modified particle swarm optimization," *Journal of Renewable and Sustainable Energy*, vol. 8, no. 1, Feb. 2016, Art. no. 015502, https://doi.org/10.1063/1.4941791.

[21] D. Oliva, E. Cuevas, and G. Pajares, "Parameter identification of solar cells using artificial bee colony optimization," *Energy*, vol. 72, pp. 93–102, Aug. 2014, https://doi.org/10.1016/j.energy.2014.05.011.

[22] W. Gong and Z. Cai, "Parameter extraction of solar cell models using repaired adaptive differential evolution," *Solar Energy*, vol. 94, pp. 209–220, Aug. 2013, https://doi.org/10.1016/j.solener.2013.05.007.

[23] A. Askarzadeh and A. Rezazadeh, "Artificial bee swarm optimization algorithm for parameters identification of solar cell models," *Applied Energy*, vol. 102, pp. 943–949, Feb. 2013, https://doi.org/10.1016/j.apenergy.2012.09.052.

[24] F. Dkhichi, B. Oukarfi, A. Fakkar, and N. Belbounaguia, "Parameter identification of solar cell model using Levenberg–Marquardt algorithm combined with simulated annealing," *Solar Energy*, vol. 110, pp. 781–788, Dec. 2014, https://doi.org/10.1016/j.solener.2014.09.033.

[25] X. Yuan, Y. He, and L. Liu, "Parameter extraction of solar cell models using chaotic asexual reproduction optimization," *Neural Computing and Applications*, vol. 26, no. 5, pp. 1227–1239, Jul. 2015, https://doi.org/10.1007/s00521-014-1795-6.

[26] A. A. Z. Diab, A. Al Sumaiti, A. A. Ezzat, A. E. Rafaat, K. A. Denis, and A. G. A. El-Magd, "New objective function of parameters extraction of photovoltaic modules for plummeting execution time complexity," *IET Renewable Power Generation*, vol. n/a, no. n/a, https://doi.org/10.1049/rpg2.12491.

[27] T. Easwarakhanthan, J. Bottin, I. Bouhouch, and C. Boutrit,, "Nonlinear Minimization Algorithm for Determining the Solar Cell Parameters with Microcomputers," *International Journal of Solar Energy*, vol. 4, no. 1, pp. 1–12, Jan. 1986, https://doi.org/10.1080/01425918608909835.